# EXPERIMENTAL INVESTIGATION OF THE VALIDITY OF AUTOMATED FIBER PLACEMENT DEFECT PREDICTIONS

Joshua Halbritter[1], Christopher Sacco[1], Alex Brasington[1], Max Kirkpatrick[1,2], Roudy Wehbe[1], Ramy Harik[1]

[1]University of South Carolina
McNAIR Center, Department of Mechanical Engineering
1000 Catawba Street
Columbia, SC 29201

[2]Siemens Digital Industries Software
5101 Westinghouse Blvd
Charlotte, NC 28273

## ABSTRACT

The utilization of advanced composites has been commonplace in the aerospace industry for many years due to their enhanced properties over generic materials. However, manufacturing of composite structures, especially large structures, continues to be challenging. A growing composite manufacturing technique for large aerospace structures is Automated Fiber Placement (AFP). Due to the increased performance and reliability of the AFP process, it has been rapidly advancing towards use on increasingly complex structures. However, these complex structures bring about their own issues, mainly the resulting unavoidable defects. These consequences can have adverse effects on the local and global laminate properties. Recent research has included predictions on the occurrence of these defects. The predictions have allowed for optimization of the process to minimize defects. Although the predictions are considered to be adequate, it is rare that they are validated with the actual manufacturing results. This paper aims to compare these predictions and simulations to real-world manufacturing results to examine their accuracy and validity leading to more integrated predictive capabilities. This is accomplished with the Computer Aided Process Planning (CAPP) software developed at the University of South Carolina's McNAIR Center. The software is used to perform process planning on a doubly curved tool to create tool paths and extract the predicted defects. Inspection results of the manufactured plies are then imported for comparison between predicted and actual defects.

Keywords: Automated Fiber Placement, Process Planning, Defects, Inspection
Corresponding author: Ramy Harik

*Copyright 2021. Used by CAMX – The Composites and Advanced Materials Expo. CAMX Conference Proceedings. Dallas, TX, October 19-21, 2021. CAMX – The Composites and Advanced Materials Expo*

# 1. INTRODUCTION

Automated Fiber Placement (AFP) is increasingly utilized for manufacturing composite materials into useful parts [1]. An AFP machine is typically comprised of a robotic arm/gantry and a fiber placement head that can layup multiple strips of fiber reinforced polymer-matrix material. These strips primarily use a carbon fiber material and are known as tows. Groups of tows, known as courses, are laid up in differently oriented layers, known as plies, to increase the strength and isotropy of the part [2]. To secure adhesion of these tows, the fiber placement head must have a method of heating the resin and compacting it down to the surface. This process is accomplished by using a controlled amount of heat and compaction load supplied by the AFP end-effector [3]. After placing the first ply on the tool surface, subsequent plies can be added until the desired thickness and strength of the part has been achieved.

During the manufacturing process, fiber defects may occur, which represent a disparity between the intended laminate design and the manufactured structure. To understand AFP defects, the source of the defect and how the part geometry influences the defect formation must be explored. A subset of these defects can be predicted and modeled through the interaction of the tool surface geometry and the fiber tows alone, while others may occur due to manufacturing conditions, machine errors, or material quality. The ability to model some of these defects enables an entire virtual layup to be built and analyzed before any manufacturing, so that those defects can be preemptively mitigated. These fiber defects can occur due to fluctuations of processing parameters such as heating and compaction, environmental factors such as temperature and humidity, or inaccurate predictions of the material's behavior that result in deviations from expected fiber placement paths.

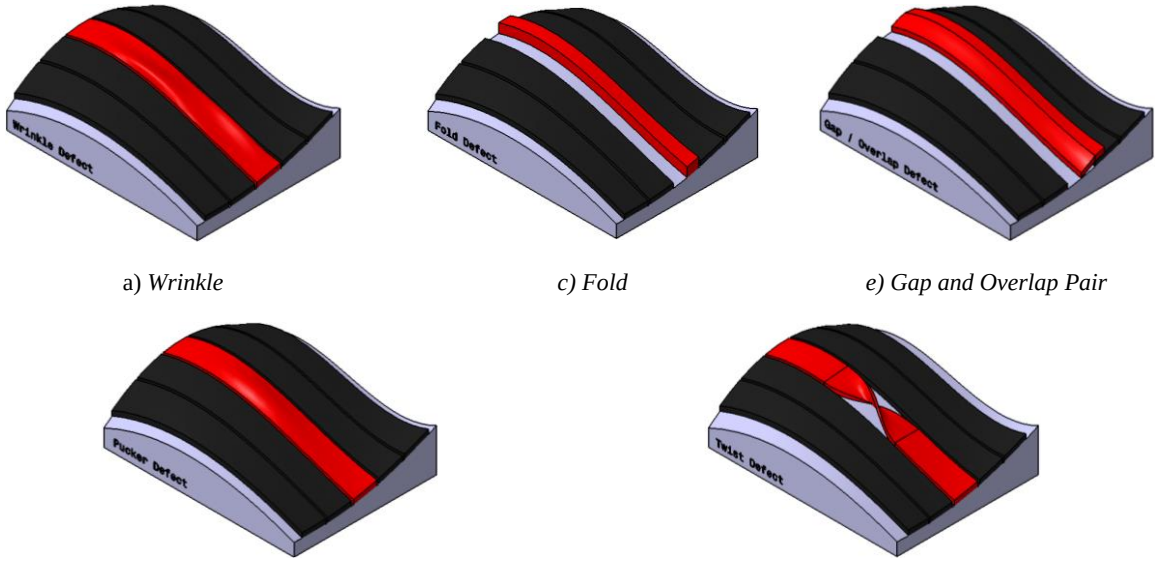


a) *Wrinkle* *c) Fold* *e) Gap and Overlap Pair*

*b) Pucker* *d) Twist*

Figure 1: Common defect types [9]

Common defect types include tow gaps and overlaps, along with fiber steering (Figure 1). When manufacturing laminates with complex surface geometries, fiber tows can no longer be placed in straight, parallel rows without excessive deformation of the tow itself. Due to the high modulus of elasticity of carbon fiber, it becomes necessary to rely on in-plane curvature of the tow placement

to minimize the overall deformation of the material. This in-plane curvature is known as fiber steering, and excessive steering can induce such defects as puckers, wrinkles, folds and twists. These resultant defects consist of out of plane deformation of the tows to reduce stresses generated from steering. Additionally, concessions must be made for the alignment of courses on complex surfaces, resulting in gaps and overlaps. A gap occurs when two adjacent tows are not perfectly laid up adjacent to each other resulting in a gap between the tows. An overlap is when the two adjacent tows are overlapping onto each other.

The prediction of defects through virtual layup, along with robust automated inspection paired with manual rework represent an efficient route for the reduction of defect occurrences and overall impact on the strength of the final composite structure [4] [5] [6]. Before the presentation of our case study, we begin with a description of the manufacturing parameters and methods used for the prediction and detected of the relevant fiber defects. The case study describes the prediction and inspection results along with a comparison of the two sets of results. Finishing with concluding remarks on the performance of defect detection and comparison along with plans for further developing the capabilities presented here.

## 2. METHODOLOGY

A sufficiently complex tool surface (Figure *2*) with a region of double curvature was selected to ensure the generation of defects for further analysis. Path planning was performed to generate a manufacturing program which consisted of 8-tow courses of 6.35mm pre-impregnated thermoset composite material. From the path planning, predictions were made for the existence and location of the primary defects, gaps, and overlaps. The fiber paths were then post-processed to include the necessary processing parameters to transition to manufacturing. The automated inspection was performed upon the completion of each ply, before continuing manufacturing.

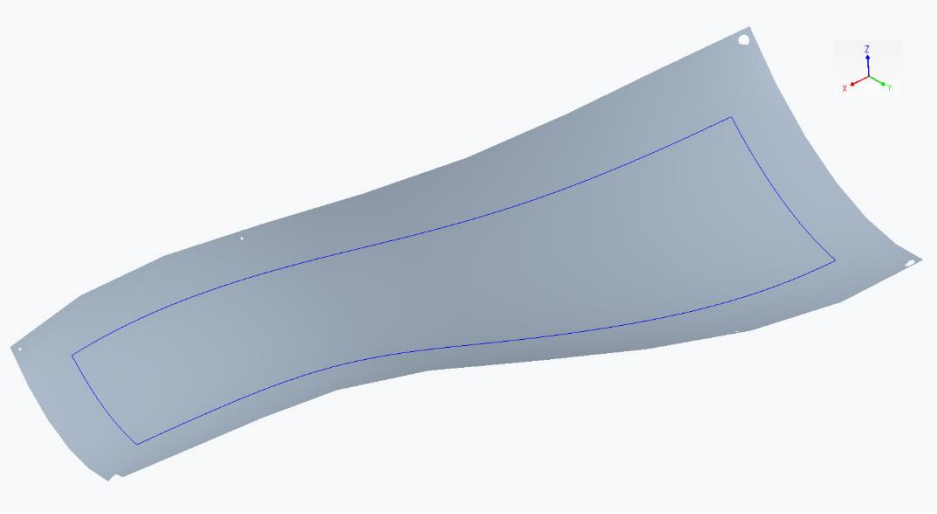

Figure 2: Complex tool surface

These steps are not novel on their own, however they have been combined into a rapid toolchain that is contained within a single environment. This allows for data gathering throughout the AFP process (design, process planning, manufacturing, inspection). Each step comes with its own information which is then combined into a dataset that is usable across multiple process domains.

This data accumulation methodology has resulted in the ability to directly compare predicted and as-manufactured defects.

### 2.1 Pre-Manufacturing Defect Prediction

The prediction of tow gaps, overlaps, angle deviations, and steering was performed with CGTech's Vericut Composite Programming (VCP) tool, which indicated the existence and location of the defects within the individual plies [7]. VCP is initially provided with the general laminate specifications to begin computing the fiber coverage. The laminate specifications indicated the extent of material coverage and primary fiber orientation for each ply. During the fiber coverage computation within each of the designated plies, the specific course paths were defined which were consistent with the fiber orientation and layup strategy. Layup strategies are key to planning fiber placement for complex surfaces, as they control individual fiber paths according to specific relationships between the surface geometry and previous fiber paths. A variety of layup strategies exist for different use cases, such as ensuring consistent fiber angle (rosette), managing fiber curvature (natural), or ensuring consistent alignment between neighboring courses (parallel) [8]. The course paths were the primary result of process planning, which are used along with machine processing parameters to create the final manufacturing program. However, the computed paths can be used to virtually reproduce the fiber placement and resulting geometry of the individual tows.

The calculation of defects directly follows the virtual reproduction of tow paths. The geometry of tows was utilized to compute the area of defects; gaps and overlaps (Figure *6*). It is important to note that gaps and overlaps were only computed between neighboring courses and not between tows within each course. The placement simulation did not include any draping or deformation of the tows that would occur during actual fiber placement, which would be necessary for the prediction of tow-to-tow interactions within courses. The resulting course to course overlaps were exported from VCP as a STEP files defining each gap and overlap instance as a unique closed surface.

### 2.2 Automated Defect Identification and Classification

Inspection of the AFP manufactured structure was accomplished through the interfacing of custom defect identification tools with the IMT developed Advanced Composite Structures Inspection System (ACSIS) [9]. ACSIS is a ply-by-ply inspection system consisting of a Kuka KR120 robotic arm actuating 4 laser profilometers. ACSIS can create rapid height profiles of a scan surface and compressing height data to create a greyscale image that can be further processed by automated detection software. After layup, the mandrel rotates the ply so that it is exposed to the ACSIS scanners. ACSIS then scans the part and processes the data as the mandrel rotates back into position for the deposition of a new ply.

ACSIS is provided with a complete software suite of defect identification tools, with the current automated detection tools for ACSIS providing patches of image that are classified as a defect or no defect. To provide more accurate defect representations, allowing for exact size and shape data to be extracted from layup scans, a custom data analysis tool was developed to aid in the inspection process. This computer vision tool is constructed from a convolutional neural network performing a semantic image segmentation task. The predicted defect pixels are then extracted and enveloped by a bounding polygon generated by the marching squares algorithm. This polygon and its

respective vertices become the basis for defect representation throughout the rest of the inspection process. This tool was built on previous defect detection software developed at the McNair Center. The software has the capability to automatically label individual pixels in an image as a given defect class, allowing for significantly more refined representation.

In addition to a more refined defect representation, the inspection software also has the capability to intake ACSIS toolpath data and reconstruct the trajectory of the scanners during inspection. Incorporating this data with the defect representations and tool geometry allow for mapping of the defects in scan images back to their original locations on the tool. It can be seen that the resulted mapping reconstructs an almost exact match to the size, shape, and location of the original defect within the tool coordinate system (Figure *3*).

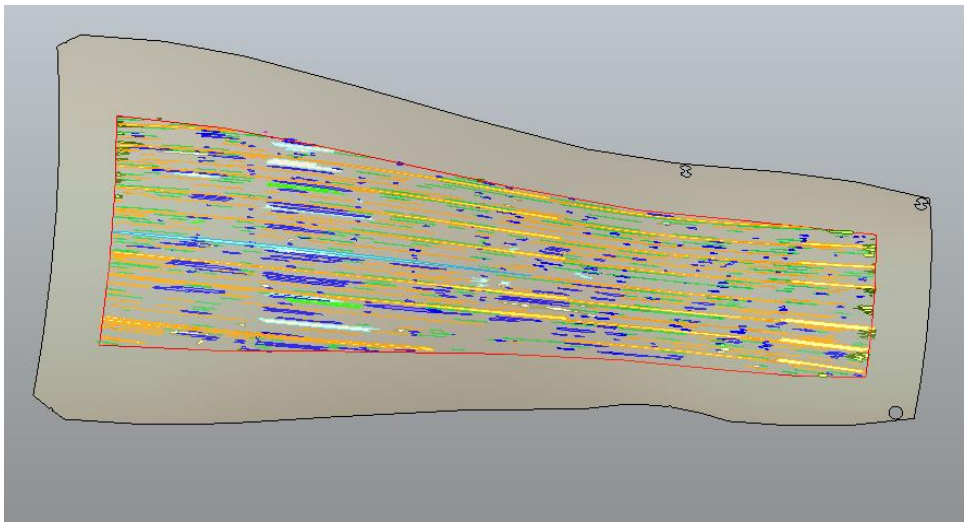

Figure 3: Defects identified through inspection and mapped onto tool surface.

This detection and classification method has the ability to separate defects into 16 categories. Table *1* below list each of these types with an associated ID and red, green, blue (RGB) color. These IDs and colors combined with the defect shapes are used to communicate the as-manufactured defect data for visualization and comparisons.

Table 1: List of defect types, IDs, and colors

| Type | ID | R | G | B | Color |
|---|---|---|---|---|---|
| No Defect | 0 | 0 | 0 | 0 | |
| Twist | 1 | 136 | 0 | 27 | |
| Fold | 2 | 247 | 249 | 165 | |
| Missing Tow | 3 | 0 | 168 | 243 | |
| Gap | 4 | 14 | 209 | 69 | |
| Overlap | 5 | 255 | 157 | 0 | |
| Wrinkle | 6 | 4 | 0 | 255 | |
| FOD | 7 | 255 | 0 | 255 | |
| Surface Separation | 8 | 153 | 153 | 102 | |
| Loose Tow End | 9 | 51 | 102 | 0 | |
| Pucker | 10 | 13 | 255 | 0 | |
| Bridging | 11 | 140 | 255 | 251 | |
| Shredders | 12 | 142 | 137 | 143 | |
| Position Error | 13 | 204 | 153 | 0 | |
| Boundary Coverage | 14 | 221 | 162 | 234 | |
| Splice | 15 | 236 | 28 | 36 | |

### 2.3 Projecting results of analysis

Both the defect predictions and inspection results are returned as boundaries and faces along the tool surface. In this format, comparison is highly difficult to accomplish programmatically due to the small size or high aspect ratio of some of the defects. This is remedied through a coordinate transformation from cartesian space to parametric u/v space (pixels system) as shown in Figure *4*. This transformation is done with the following steps:

1. An empty high-resolution array of pixels is created with the array's size being dependent on the maximum u and v parameters of the tool surface.

2. The boundary of individual defects are projected onto the surface to be represented in u/v space.

3. The projected boundaries are discretized into high fidelity polygons and filled with its associated color (Table *1*) to produce the defect area in the pixel array.

4. Step 2 is repeated for each defect present in the current ply.

5. The final array of color pixels is then saved as a PNG file for later use.

6. Steps 1-5 are repeated for each defect type for predicted and as-manufactured defects.

The representation of the defects through the pixel system facilitates faster and more accurate computation of boolean operations between different defect sources and surface areas resulting from those operations.

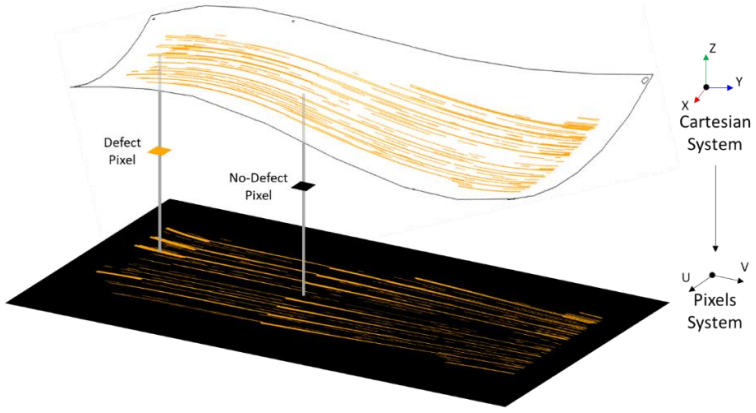


Figure 4: Projection of surface defects

# 3. CASE STUDIES

For experimentation, a zero-degree ply angle was used with the ply boundary and starting point shown in Figure 5a, combined with a Rosette Rule layup strategy. This information was then used to manufacture the zero-degree ply Figure 5b. The following section details the data collected from both the defect predictions and the inspection results.


Figure 5:Tool surface with a) Description of process planning information; b) Resulting manufactured 0° ply

## 3.1 Defect Predictions

The zero-degree ply was processed through VCP to generate the defect predictions. A total of 8 tows were utilized for each course to match the manufacturing capabilities. The maximum course to course gap was set to 0mm and a maximum overlap of 6.35mm (one tow width). These settings ensured the presence of material overlap while preventing gaps. Those settings enabled the comparison of predictions and inspection for overlaps, while ensuring the present of any gaps would occur as a result of manufacturing processes and would only be detected by the inspection.

Following generation of the course paths and individual tow geometry, the defect analysis was performed for gaps, overlaps, and angle deviation.

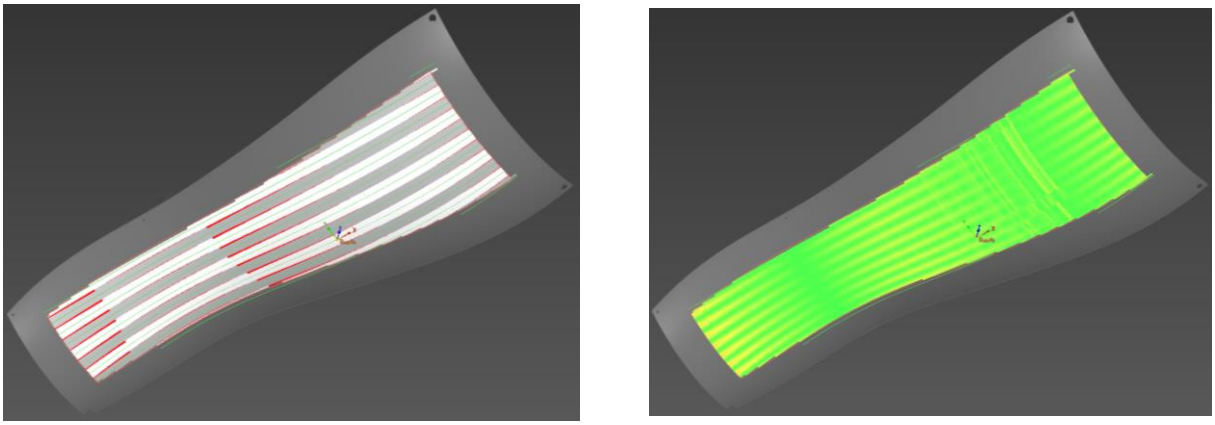

Figure 6: VCP Analysis a) Overlaps(red); b) Angle Deviations (yellow)

No tow gaps were detected during the defect analysis. However, tow overlaps and angle deviation were detected extensively through the divergent regions of the tool surface. The overlaps (Figure *6*a) depicted in red, exist between the neighboring courses, alternatingly depicted in white and gray. Fiber angle deviations (Figure *6*b) are depicted on a continuous spectrum, where green represents little to no deviation, while yellow represents 3-4° of fiber angle deviation. The defects were then converted to the discretized pixel representation for further investigation (Figure *4*).

### 3.2 Defect Inspection

Following the placement of the zero-degree ply, the ACSIS profilometry inspection was performed. Through the inspection process a total of 8 defect types were extracted (missing tow, gap, overlap, pucker, wrinkle, surface separation, loose tow, and bridging). The inspection was programmed to replicate the manufacturing motion in order to scan the individual courses. The profilometry data was then stitched together to generate a unified scan of the ply to finally generate the labeled defect data. These defects were referenced back to the tool surface and then pixelated, using the previously defined method, resulting in the images in Figure *7*.

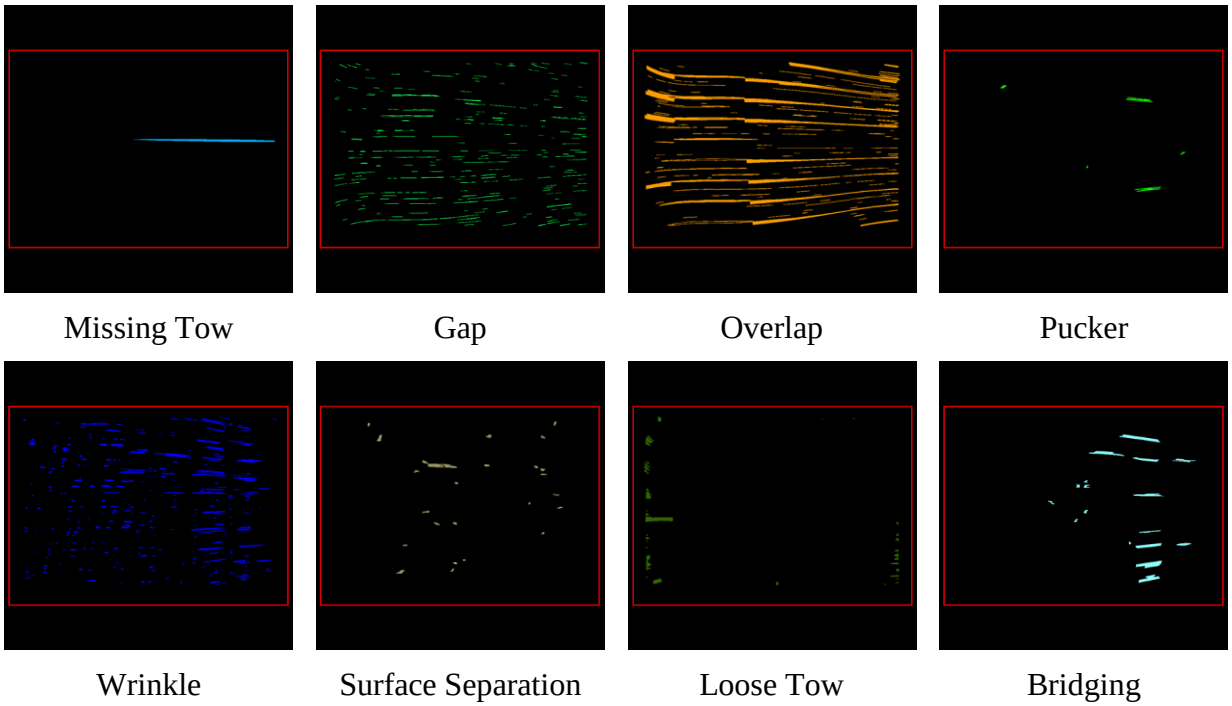


Figure 7: Images of the pixelated defects of each type found during processing of inspection data

### 3.3 Comparison of Predicted and Detected Defects

The comparison of the predicted and detected defects were performed using the pixelated data generated through the methods outlined in section 2.3. The projections mapped the defects back to the individual faces of the CAD model, however the tool surface utilized only had a single face.

The comparison of the predicted and actual overlaps is presented in Figure 8. The predicted overlaps (red) correspond to the edge of neighboring courses, whereas the actual overlaps (blue) were measured over the entire ply and thus detected overlaps between tows within individual courses as well as the overlaps between courses. It is important to note that the prediction of gaps and overlaps were limited to simple geometric models, whereas prediction of tow-tow interactions may require more detailed models to account for tow deformation over the tool surface during placement.

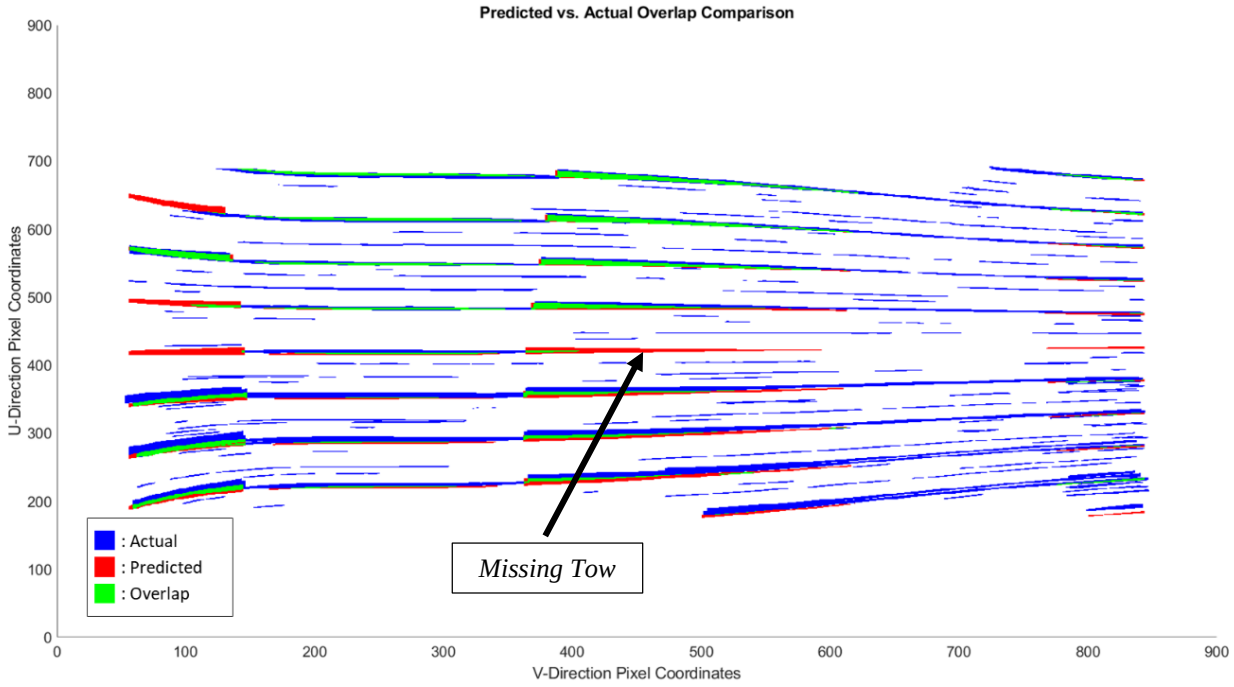


Figure 8: Comparisons of predicted and actual overlaps

Table 2: Comparisons of overlap defect areas

| **Overlap Defect Area Comparisons** | | |
|---|---|---|
| Predicted area | 55001.6 | $mm^2$ |
| Actual area | 67717.9 | $mm^2$ |
| Error | 18.8% | |

Another possible reason for mismatch between the predicted and measured overlaps is the development of other types of defects in that region during manufacturing and their capture and labeling under another type of defect during inspection. For instance, the occurrence of a missing tow where a gap was predicted to occur can result in such discrepancy. The same applies to out-of-plane defects such as puckers, wrinkles, surface separation, and bridging, where a "designed" overlap could possibly act as an instigator for such defects. As a result of this difference in capabilities between prediction and actual inspection, the actual overlap area was approximately 23% greater than the predicted area (Table 2).

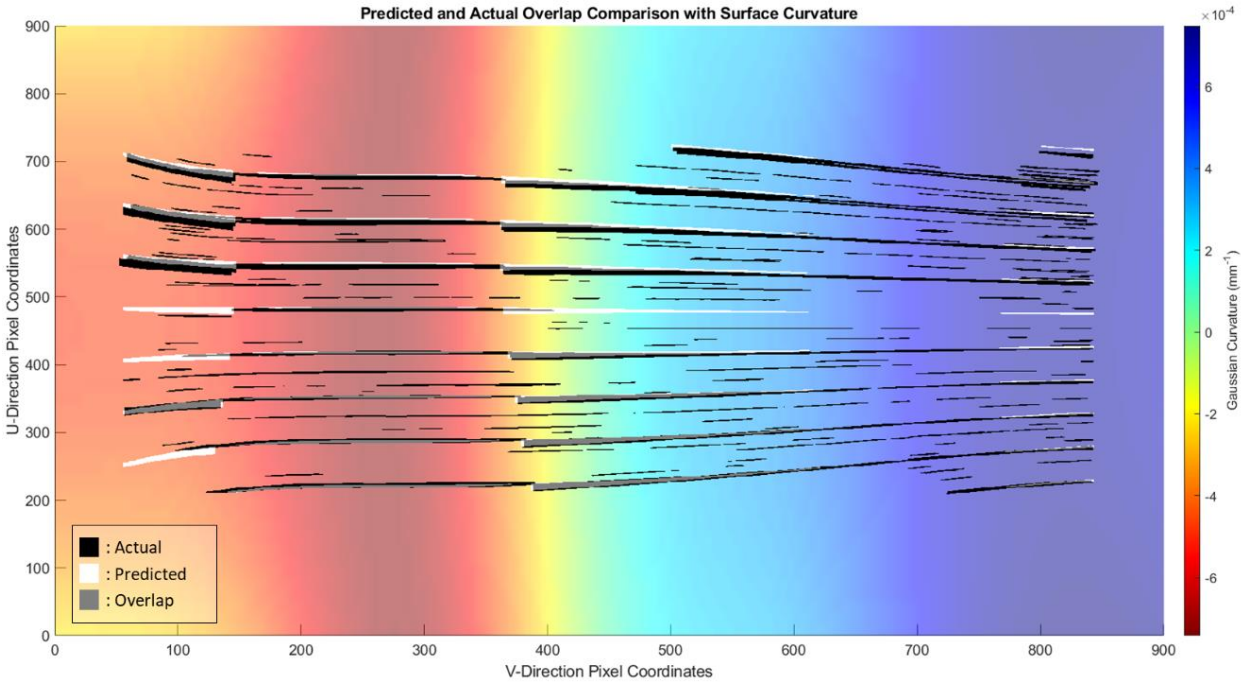


Figure 9: Comparisons of predicted and actual overlaps combined with surface curvature

Additionally, the results of the predicted and actual defects were overlayed onto the curvature of the surface (Figure 9). The extent of the defects closely matches the curvature of the surface, where sets of defects are delineated at the changes of curvature. These results reflect on the modification of tow count and course direction in order to meet the gap and overlap settings that were utilized.

## 4. DISCUSSION

We have presented an efficient toolchain for the comparison of fiber defects from various sources. The approach relies heavily on the accurate CAD representation of the tool surface, and the ability to digitally capture and predict defects and map them back to the tool surface. The digitized defects can then be discretized according to the tool surface geometry, allowing for further evaluation of the defect capture sources. The case study presented here focused on the prediction and inspection results for the overlap defect but can be expanded to other defect types relating back to tow geometry. The ply geometry and overlap prediction were performed through VCP and CAPP, and the manufactured ply was inspected with ACSIS.

The ability to accurately map and compare defect instances and severity back to the digital tool surface can greatly benefit the overall understanding of fiber defects during manufacturing and process planning. Through the understanding of the fiber defects and their origins, designers can accurately design composite structures around manufacturing capabilities. This can significantly enhance the application of AFP to larger and more complex composite structures and reduce the time from design to manufacturing.

### 4.1 Future Work

The comparison of defects provides a two-fold benefit, where each defect detection method can be used to augment the other. Simple geometric defect detection provides the ability to identify many problematic defects before any manufacturing occurs and enables modification of ply coverage to correct for those defects. Whereas post manufacturing inspection techniques can identify and classify defects regardless of source but requires an iterative design and manufacturing cycle to eliminate defects induced by the originally planned laminate design. The combination of these two systems could be used to more accurately predict and model defects before they appear during manufacturing trials, and the prediction of defects can be used during the training of defect inspection systems. Additionally, the comparison of defects should expand into more complex defect classes, particularly those which derive from fiber steering [10], which is a necessary process to manufacture the increasing complex structures required by industry.

## 5. ACKNOWLEDGMENT

The authors would like to thank Toray Composite Materials America, Inc. for supplying the materials used in the presented experimentation. Also, the authors would like to thank Ingersoll Machine Tools, Inc. for the usage of software and equipment used during the experiments.

## 6. REFERENCES

[1] H. J. L. Dirk, C. Ward and D. K. Potter, "The engineering aspects of automated prepreg layup: History, present and future," *Composites Part B: Engineering*, vol. 43, no. 3, pp. 997-1009, 2012.

[2] K. Croft, L. Lessard, D. Pasini, M. Hojjati, J. Chen and Yousefpur, "Experimental study of the effect of automated fiber placement induced defects on performance of composite laminates," *Composites Part A: Applied Science and Manufacturing*, vol. 42, no. 5, pp. 484-491, 2011.

[3] P. Debout, H. Chanal and E. Duc, "Tool path smoothing of a redundant machine: Application to Automated Fiber Placement," *Computer-Aided Design*, vol. 43, pp. 122-132, 2 2011.

[4] K. Fayazbakhsh, M. A. Nik, D. Pasini and L. Lessard, "Defect layer method to capture effect of gaps and overlaps in variable stiffness laminates made by Automated Fiber Placement," *Composite Structures,* vol. 97, pp. 245-251, 3 2013.

[5] M. Lan, D. Cartié, P. Davies and C. Baley, "Influence of embedded gap and overlap fiber placement defects on the microstructure and shear and compression properties of carbon–epoxy laminates," *Composites Part A: Applied Science and Manufacturing,* vol. 82, pp. 198-207, 3 2016.

[6] A. Sawicki and P. Minguett, "The effect of intraply overlaps and gaps upon the compression strength of composite laminates," in *39th AIAA/ASME/ASCE/AHS/ASC Structures, Structural Dynamics, and Materials Conference and Exhibit*, 1998.

[7] CGTech, *VERICUT Composite Programming,* 2021.

[8] G. Rousseau, R. Wehbe, J. Halbritter and R. Harik, "Automated Fiber Placement Path Planning: A state-of-the-art review," *Computer-Aided Design and Applications,* vol. 16, p. 172–203, 8 2018.

[9] C. Sacco, A. B. Radwan, A. Anderson, R. Harik and E. Gregory, "Machine learning in composites manufacturing: A case study of Automated Fiber Placement inspection," *Composite Structures,* vol. 250, p. 112514, 10 2020.

[10] R. Wehbe, "Modeling of Tow Wrinkling in Automated Fiber Placement based on Geometrical Considerations," *University of South Carolina,* 2017.

[11] R. Harik, C. Saidy, S. J. Williams, Z. Gurdal and B. Grimsley, "Automated fiber placement defect identity cards: cause, anticipation, existence, significance, and progression," in *SAMPE 18,* Long Beach, CA, 2017.